

Device-independent, high bit-rate quantum random number generator with beam-splitter-free architecture and live Bell test certification

Ayan Kumar Nai, Vimlesh Kumar, G. K. Samanta

Ayan Kumar Nai

Photonic Sciences Lab., Physical Research Laboratory, Ahmedabad 380009, Gujarat, India

Indian Institute of Technology Gandhinagar, Ahmedabad 382424, Gujarat, India

Email Address: ayankrnai@gmail.com

Vimlesh Kumar, G. K. Samanta

Photonic Sciences Lab., Physical Research Laboratory, Ahmedabad 380009, Gujarat, India

Keywords: *QRNG, Entangled photon source, Bell parameter, Entropy, Toeplitz, NIST, Auto-correlation*

We present a beam-splitter-free, high-bit rate, device-independent quantum random number generator (DI-QRNG) with real-time quantumness certification via live Bell test data. Using a 20-mm-long, type-0 phase-matched PPKTP crystal in a polarization Sagnac interferometer, we generated degenerate, non-collinear parametric down-converted entangled photons at 810 nm in an annular ring distribution with pair photons appearing at diametrically opposite points on the ring randomly. Dividing the ring into six sections and collecting photons from opposite sections, we developed three entangled photon sources from a single resource (optics, laser, and nonlinear crystal). Using a pump power of 12.4 mW at 405 nm, we recorded coincidence (1 ns window) timestamps of any two sources without projection to assign random bits (0 and 1) while measuring the Bell parameter ($S > 2$) with the third source for live quantumness certification. We have generated 90 million raw bits in 46.4 seconds, with a minimum entropy extraction ratio exceeding 97%. Post-processed using a Toeplitz matrix, the QRNG achieved a 1.8 Mbps bit rate, passing all NIST 800-22 and TestU01 tests. Increasing the coincidence window to 2 ns boosts the bit rate to over 2 Mbps, maintaining minimum entropy above 95% but reducing the Bell parameter to $S = 1.73$. This novel scalable scheme eliminates beam splitters, enabling robust, multi-bit DI-QRNG with enhanced ring sectioning and trustworthy certification for practical high-rate applications.

1 Introduction

Random numbers play a fundamental role in a wide range of applications, including cryptographic protocols, secure communication, and scientific simulations [1, 2]. The random numbers generated through the deterministic classical computer algorithms, known as the pseudo-random number generators (PRNGs), are vulnerable to predictability and external tampering [3, 4]. On the other hand, the random numbers generated by exploiting the inherent unpredictability of quantum stochastic process, known as the quantum random number generators (QRNGs), guarantee the generation of truly random numbers [5, 6]. Typically, the quantum stochastic process includes the measurement of quantum-phase fluctuation, single photon detection, and vacuum fluctuations [7–9]. Conventionally, the QRNGs have two parts: source (generating quantum states inherently random) and measurement (demolition of quantum state using a practical device such as a beam splitter and subsequent detection using a detector to generate raw bits). However, in the absence

of perfect devices for generation and measurement, practical QRNGs can suffer from security loopholes, leading to the development of device-independent QRNGs (DI-QRNGs) independent of the physical implementation and characterization of the instruments used [10–12]. Typically, the DI-QRNGs have the inherent certification of randomness based solely on the violation of Clauser-Horne-Shimony-Holt (CHSH) form of Bell’s inequality [13] without assuming trust in the internal workings of the quantum random number generation scheme [14, 15]. Despite having the highest security in the random numbers, the DI-QRNGs have a relatively lower bit rate [14, 16] due to the limitations on the brightness of the entangled sources developed using the current technologies. As a result, the practical implementations of DI-QRNGs parallel with the QRNG scheme have not been explored yet. Alternatively, efforts have been made to enhance the bit rate of the QRNG through exploration of different protocols such as source-independent QRNG [17–20], measurement device-independent QRNG [21, 22], and semi-device independent QRNG [23, 24] with different as-

assumptions about the source or the measurement at the cost of ultimate security of the randomness. Additionally, the device-independent QRNGs are not loss tolerant, demanding very severe requirements on experimental devices. On the other hand, the majority of the QRNGs often rely on physical devices such as 50:50 beam splitters or polarization beam splitters, despite the technological challenge of making a perfect lossless, unbiased beam splitter.

Therefore, it is imperative to devise new protocols for the development of DI-QRNG with a high bit rate while ensuring randomness by the intrinsically probabilistic nature of quantum physics. Recent advancements in quantum optics and engineering have opened pathways to simplify DI-QRNG architectures. Beam-splitter-free designs are particularly promising, offering streamlined setups that reduce complexity and enhance robustness [20, 25, 26]. Additionally, incorporating real-time randomness certification, such as live Bell test verification, strengthens the trustworthiness of the generated numbers by providing immediate validation of the CHSH inequality [13] for the source.

In this paper, we introduce a novel beam-splitter-free, high-bit rate DI-QRNG with live Bell test certification. Using the non-collinear, degenerate, spontaneous parametric downconversion (SPDC) process of a 20-mm long periodically-poled potassium titanyl phosphate (PPKTP) crystal in a polarization Sagnac interferometer, we have developed three high-brightness entangled photon sources [27, 28] from the single resources (optical components, nonlinear crystal, and laser source) by dividing the SPDC ring into six diametrically opposite sections. Since the generation of the pair-photons over the diametrically opposite points of the SPDC ring is purely random and governed by the quantum mechanical process, we have generated random bits (raw) with min-entropy exceeding 97% by measuring the coincidence of the quantum correlated pair photons of the two entangled photon sources without any projection and third source for live measurement of CHSH Bell's parameter ensuring real-time trustworthiness of the source confirming the development of DI-QRNG. The entropy ensures high efficiency in extracting true random bits. Using Toeplitz matrix-based post-processing, our DI-QRNG system results in a bit rate of 1.8 Mbps, passing all NIST 800-22 and TestU01 statistical test suites. Such a generic experimental scheme can be scalable to provide a higher bit rate through the generation of a multi-bit DI-

QRNG system with live certification by dividing the SPDC ring to form more entangled photon sources from the single resource.

2 Experiment

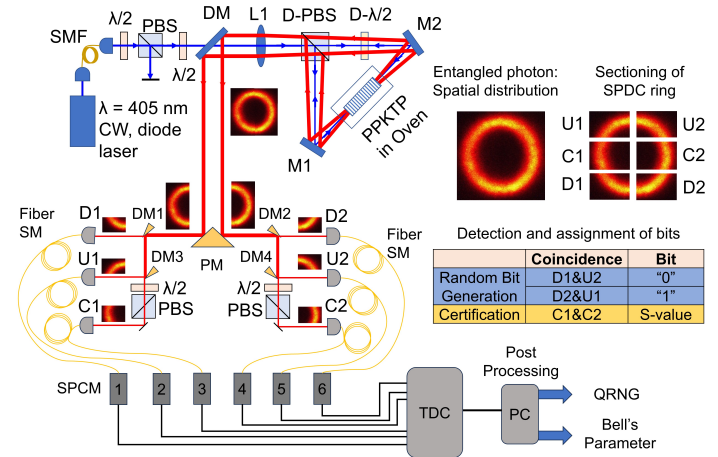


Figure 1: The schematic representation of (a) (b) the experimental setup of the QRNG source. Laser: 405 nm, cw diode laser, $\lambda/2$: Half wave plate, L1: plano-convex lenses of focal length 150 mm, D – $\lambda/2$: Dual Half wave plate, PPKTP: 20 mm long PPKTP crystal of single grating period in temperature oven, IF: Interference filter, PM: Prism shaped gold coated mirror, DM1-4: D-shaped mirrors, U1-2, D1-2 and S1-2: Upper, lower and sider sections of the SPDC ring, SM: Single-mode fiber, SPCM1-6: single photon counting modules, TDC: Time-to-digital converter, PC: Computer. and (b) the concept of simultaneous EP and QRNG source.

The schematic of the experimental setup for the device-independent QRNG system with live CHSH Bell's parameter measurement is illustrated in Fig. 1. A continuous-wave, single-frequency (linewidth ~ 20 MHz), single-mode fiber (SMF)-coupled laser diode providing an output power of 21 mW at a central wavelength of 405 nm is used as the pump source. Operating the laser at its highest power to ensure optimum performance, the power attenuator, comprised of a half-wave plate ($\lambda/2$) and a polarizing beam splitter (PBS) cube, is used to control the input pump power to the experiment. A second $\lambda/2$ plate is used to control the polarization state of the linearly polarized pump beam to balance the laser power in both clockwise (CW) and counterclockwise (CCW) beams of the polarization Sagnac interferometer, which consists of a dual-wavelength PBS (D-PBS, for 405 and 810 nm) and two plane mirrors, M1 and M2. The lens, L1, with a focal length of $f = 150$ mm, focuses the pump beam with a spot size of $\sim 40 \mu\text{m}$ at the center of the nonlinear crystal placed

between mirrors M1 and M2. The dual-wavelength half-wave plate ($D-\lambda/2$), with its optic axis rotated by 45° relative to the vertical, is placed inside the Sagnac interferometer to transform horizontal polarization to vertical and vice versa for both 405 nm and 810 nm wavelengths. A single grating (grating period $\Lambda = 3.425 \mu\text{m}$) periodically-poled potassium titanyl phosphate (PPKTP) crystal with a length of 20 mm and a $1 \times 2 \text{ mm}^2$ aperture serves as the nonlinear medium, producing degenerate SPDC photons at 810 nm through non-collinear, type-0 ($e \rightarrow e + e$) phase-matching. The crystal is housed in an oven with a temperature range up to 200°C and a stability of $\pm 0.1^\circ\text{C}$.

The CW and CCW pump beams, in the presence of the $D-\lambda/2$ plate, generate pair photons distributed in an annular ring with orthogonal polarization states. When superimposed on the D-PBS, the SPDC photons exhibit an annular ring distribution, with pairs of photons located at diametrically opposite points on the ring and described by the state, $\psi = (HH+VV)/\sqrt{2}$ (a Bell state). The SPDC photons are collimated by lens L1 and separated from the pump beam by a dichroic mirror (DM) positioned between lens L1 and the $\lambda/2$ plate. The collimated annular SPDC ring, as observed by the EMCCD camera (Andor, iXon Ultra 897) with an interference filter of bandwidth $\sim 3.2 \text{ nm}$ centered at 810 nm, is shown by the image in the inset of Fig. 1.

We divided the SPDC into two halves by the gold-coated prism mirror (PM), and subsequently, each half is divided into three subsections by D-shaped mirrors, DM1-4, resulting in three pairs of diametrically opposite sections (U1, D2), (U2, D1) and (C1, C2) having pair photons. While the photons from each section are collected using the combination of an interference filter (bandwidth of 3 nm) mounted fiber coupler, single-mode fiber (SM), and single photon counting modules, SPCM1-6, (SPCM-AQRH-14-FC), the photons of sections C1 and C2, passes through the polarization analyzer consists of a $\lambda/2$ plane and PBS before collection. The time-to-digital converter (TDC) (MultiHarp 150, PicoQuant) is connected to the SPCMs, and the computer is used for photon counting, time stamping, recording, and experimental data analysis. The three pairs of diametrically positive sections of the annular ring form the three sets of single/entangled photon sources. For raw bit generation, as shown by the table of Fig. 1, we assign bits “0” and “1” for the coincidence event between the photons of sec-

tions (D1 & U2) and (D2 & U1), respectively. As the appearance of photon pairs in sections (U1, D2) and (U2, D1) are quantum mechanically random, this method produces a sequence of random bits of 0 and 1. The photons of sections (C1 and C2) are used for the entanglement study of the pair photons through the polarization projective measurement and Bell’s parameter calculation. The coincidence window throughout the manuscript, if otherwise mentioned, is 1 ns.

3 Results and discussions

We first characterized the entangled photon source by measuring the interference visibility in different bases and the value of Bell parameters as a function of pump power and coincidence window. Using the pair photons from the sections (C1, C2), we have set the polarization state of one of the photons (say from C2) at horizontal (H), vertical (V), diagonal (D), and anti-diagonal (A) using the $\lambda/2$ plane and measured the interference visibility, $V = (\text{max.} - \text{min.}) / (\text{max.} + \text{min.})$, by recording the coincidence counts while continuously rotating the polarization state of the other photon (from C1) using $\lambda/2$. The visibility for different bases as a function of pump power is shown in Fig. 2. As evident from Fig. 2(a), the entanglement visibility in all bases (H, V, D, and A) are almost comparable for each pump power, however, with the increase of pump power from 0.5 mW to 12.4 mW and coincidence window of 1 ns, the visibility decreases from 97% to 73%, respectively. However, the interference visibility, $> 71\%$, for all power levels confirms the entanglement [27]. Further, keeping the pump power constant at 12.4 mW, we measured the interference visibility further decreasing from 73% to 61%, below the 71% limit to ensure entanglement, with the increase of coincidence window from 1 ns to 2 ns with a step of 0.5 ns. The measurement of Bell’s parameter, S , as shown in Fig. 2(b), confirms the decrease of S-value from 2.73 to 2.07 with the pump power increase from 0.5 mW to 12.4 mW. Although $S \geq 2$ confirms the entanglement, the increase of the coincidence window from 1 ns to 2 ns drastically reduces the S-value from 2.07 to 1.73 due to the generation of multiphotons at high pump power and detection of such photons in the presence of longer coincidence window ($> 1 \text{ ns}$). Such observation confirms the control transition of the output of the pair photon source from the quantum state to the classical two-photon

state. As expected, we observe similar performance of the pair photons collected from the sections (U1, D2) and (U2, D1), confirming the development of three entangled photon sources from a single set of resources (laser and crystal). In fact, by dividing the annular ring of the photons into more pairs, one can develop a larger number of entangled photon sources; however, this comes at the cost of reduced brightness.

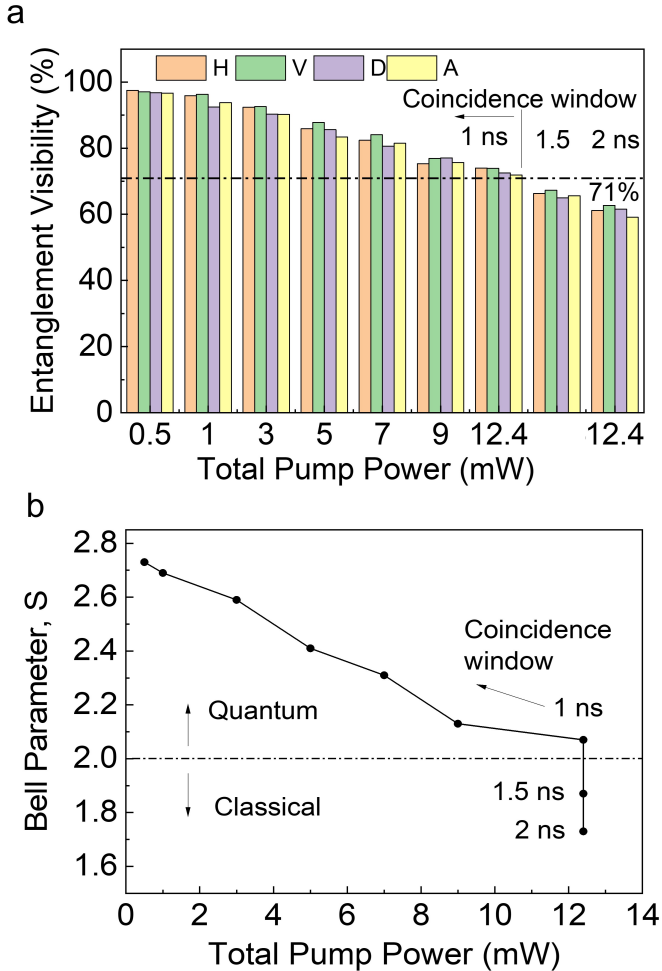


Figure 2: Variation of (a) Entanglement visibility and (b) Bell parameter (S) of the entangled photon source as a function of pump power and with coincidence window

Knowing the performance metrics of the entangled photon source as a function of input power, we recorded the time stamps of the coincidence counts for photon pairs collected from the sections (U1 & D2) and (U2 & D1) and assigned binary values of 0 and 1, respectively, while simultaneously checking the Bell parameter of the source using the sections (C1 & C2) (see Fig. 1). Subsequently, we recorded over 90 million raw bit sequences of 0's and 1's for each pump power. Due to the dependence of pump

power on the generation rate of photon pairs, the recording time for 90 million bits decreased with increasing pump power, resulting in a recording time of 46.4 seconds at 12.4 mW of pump power for a coincidence window of 1 ns. Since the raw bit sequences contained all possible errors, we calculated the minimum entropy [7, 29] as mentioned in our previous report [20] to estimate the maximum extractable unbiased true random bits. The results, presented in Fig. 3, show that the min-entropy, $H_\infty(X)$ (black squares), remained nearly constant in the range of 99% to 97% as the pump power increased from 0.5 mW to 12.4 mW. For the increase of the coincidence window from 1 ns to 2 ns at a fixed pump power of 12.4 mW, the Bell parameter, S , decreased from 2.07 to 1.73 (see Fig. 2(b)), indicating the loss of entanglement. However, it is interesting to note that there is no significant change in the min-entropy, $H_\infty(X)$, value even for $S < 2$.

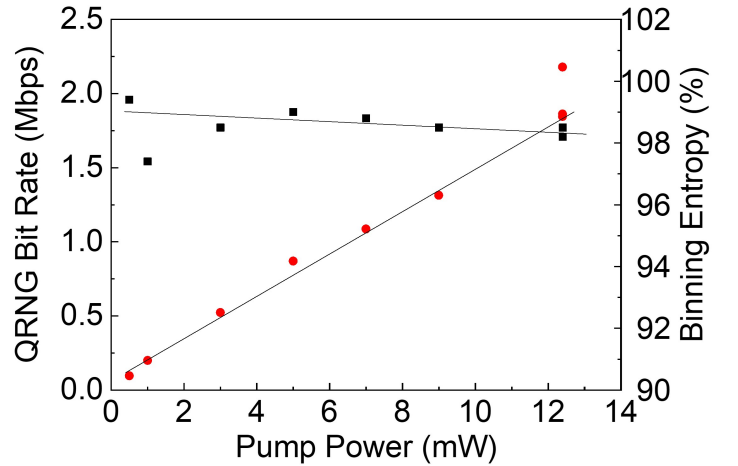


Figure 3: The variation of the minimum entropy, $H_\infty(X)$ (black dots), and post-processed QRNG bit rate (red dots) as a function of pump power and $g^{(2)}(0)$. The solid lines (red and black) are linear lines fit to the experimental data.

Such observation demonstrates that the reduction in min-entropy is primarily due to classical noise in the experimental setup and is independent of the entanglement quality of the quantum source. To distill true random bits from the raw bit sequences, we employed a Toeplitz hashing randomness extractor [30]. The post-processed QRNG bit rate (red dots in Fig. 3) exhibited a linear increase with pump power, rising from 0.09 Mbps at 0.5 mW to 1.8 Mbps at 12.4 mW, corresponding to a slope of 0.14 Mbps per mW. Additionally, at 12.4 mW pump power, increasing the coincidence window from 1 ns to 2 ns boosted the bit rate from 1.84 Mbps to 2.18

Mbps. These results confirm the development of a high bit rate, device-independent QRNG system offering simultaneous Bell parameter measurement. Again, the higher value of min-entropy, $H_\infty(X)$, confirms the possibility for further enhancement of the bit rate of the device-independent QRNG system to a few tens of Mbps by simply increasing the pump power or by increasing the coincidence window. However, due to the unavailability of a higher power pump laser at 405 nm, we restricted the bit rate to 2.18 Mbps. Unlike our previous report [20], the lower bit QRNG rate in the current experiment can be attributed to the larger ring diameter of the pair photons to make easy division into six sections and lower effective power to the crystal.

the bit sequence, we calculated the uniformity of the P-values and the proportionality test to find the proportion of the input sequences passing (P-value is above the chosen significance level, α , usually $\alpha = 0.01$) a test. Using the Goodness-of-Fit distributional test and Kolmogorov-Smirnov tests to the post-processed bits, we calculated the final P-values of 15 different tests under the NIST test suite of the post-processed bits at visibilities, $V = 95\%$ (green) and $V = 61\%$ (orange) with the results shown in Fig. 4. As evident from Fig. 4, the P-values of all the tests are > 0.01 , confirming the randomness of the experimental results at the different visibility levels. Although we have 80 sequences of bit strings, each consisting of 1 million bits for both entanglement visibilities of the quantum source, the NIST statistical test suite randomly selected $n = 46$ sequences for the random excursions and random excursion variant tests. For these tests, using a significance level of $\alpha = 0.01$ and $n = 46$, the proportional fraction range was calculated to be (0.946, 1.034). For the remaining tests, with $\alpha = 0.01$ and $n = 80$, the proportional fraction range was determined to be (0.956, 1.023). We observed that the proportional fractions for all post-processed bit sequences fell within these specified ranges, confirming successful results across all tests and demonstrating the randomness of the generated bit sequences.

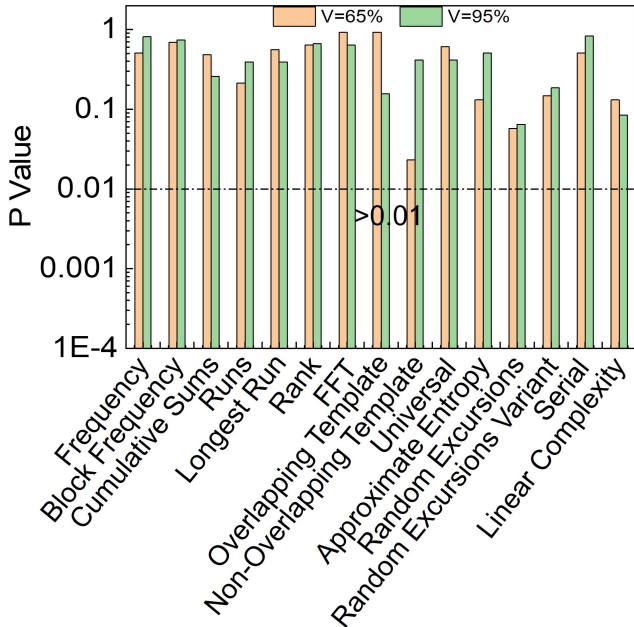


Figure 4: Final P-values of 15 tests under NIST statistical suit for the Toeplitz post-processed bits recorded at 95% and 61% visibility, respectively.

To estimate the quality of randomness, we used the NIST 800-22 Statistical Test Suite [31] to the post-processed bit strings derived from the entangled photons with two different levels of entanglement visibility, $V = 95\%$ and $V = 65\%$. For each visibility setting, we have divided the bit string into 80 sequences of binary bits, similar to our previous work [20], each containing one million bits, thereby exceeding the minimum requirement of 55 sequences as recommended by the NIST test suite. As the NIST statistical test suite follows two primary types of quantification to determine the randomness of

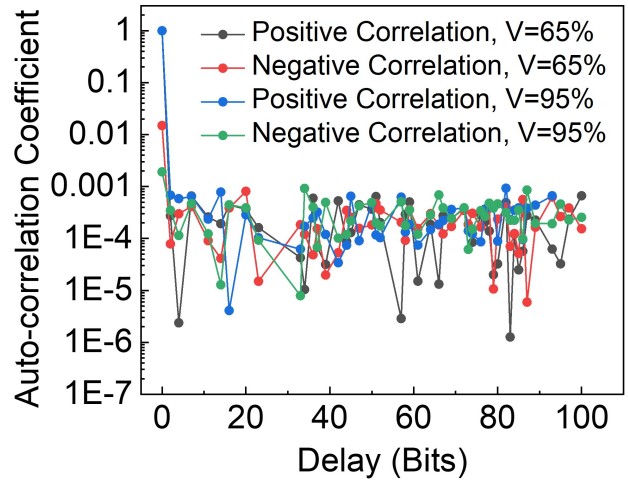


Figure 5: Variation of the magnitude of the positive and negative autocorrelation coefficients of the first 10 million bits of the raw bit sequence up to a delay of 100 bits. The raw bit sequence is recorded at the visibilities of .

Further, we evaluated the randomness of our post-processed bits using the TestU01 statistical test

suite, specifically the Rabbit, Alhabit, and Block-Alhabit battery tests. While these tests typically require sequences of approximately 30 million bits, we employed longer sequences of 80 million bits for more rigorous analysis. Following the methodology outlined in the literature [32,33], we interpreted the P-values by considering values within the interval $[10^{-3}, 1 - 10^{-3}]$ as a success, and value outside this interval as a failure. We observed the P values for the post-processed bit string successfully passed all three tests, indicating the validation of our novel experimental scheme.

We further analyzed the randomness of the raw bits for two different entanglement visibilities, $V = 95\%$ (quantum state) and $V = 61\%$ (classical states), by calculating the autocorrelation coefficient. Using the first 10 million bits of the raw bit sequence, we computed the autocorrelation coefficient up to a delay of 100 bits, as shown in Fig. 5. It is evident from Fig. 5 that even after a delay of 100 bits, the mean and standard deviation of the autocorrelation coefficient remain nearly unchanged. Given that a truly random sequence has an autocorrelation coefficient with a mean value close to zero, in our experiment, the raw bits for both entanglement visibilities exhibited a minimum autocorrelation coefficient in the order of $\sim 10^{-6}$ and a standard deviation of 9.8×10^{-4} . Such low values of minimum autocorrelation coefficient confirm that the raw bit string generated using the source of the entangled photons in the current novel experimental scheme represents a good random sequence even before post-processing, leading to a high min-entropy, $H_\infty(X)$ as shown in Fig. 3, and enabling efficient extraction of high-quality random bits.

4 Conclusions

We successfully demonstrated a novel beam-splitter-free, high-bit-rate DI-QRNG system with simultaneous quantumness certification through live Bell test data. The randomness is derived from direct access to the random occurrence of photon pairs at diametrically opposite points on the annular ring distribution of entangled photons, generated via a noncollinear degenerate SPDC process in a type-0 phase-matched PPKTP crystal within a polarization Sagnac interferometer. At a pump power of 12.4 mW and a 1 ns coincidence window, we achieved an entanglement visibility of $\sim 73\%$ and a Bell parameter, $S = 2.07$, and recorded high-quality quan-

tum random bits 90 million of raw bits with $>97\%$ minimum entropy, which is further confirmed by an autocorrelation coefficient ($\sim 10^{-6}$). Toeplitz post-processing verified the QRNG of a bit rate of 1.8 Mbps, passing all NIST and TestU01 test suites. Notably, increasing the coincidence window to 2 ns reduced visibility to 61% and the Bell parameter to $S = 1.73$ but produced raw bits has minimum entropy $>95\%$ and a post-processed QRNG bit rate of 2.18 Mbps. Although we have divided the annular ring of the pair photons into six sections, forming three high-brightness entangled photon sources from a single resource (laser, nonlinear crystal, and optical elements) for QRNG and live Bell's test, the generic experimental scheme can in principle be used to create more sections of the SPDC ring to form more number of entangled photon sources to increase the bit-rate of the Di-QRNG and for other advance quantum networks. The novel design simplifies the technical requirements of the DI-QRNGs and sets a new benchmark for the trustworthiness of the generated random numbers for real-world applications.

ACKNOWLEDGMENTS

A. K. N., V. K., and G. K. S. acknowledge the support of the Department of Space, Govt. of India. A. K. N. acknowledges funding support for Chanakya - PhD fellowship from the National Mission on Interdisciplinary Cyber-Physical Systems of the Department of Science and Technology, Govt. of India through the I-HUB Quantum Technology Foundation. G. K. S. acknowledges the support of the Department of Science and Technology, Govt. of India, through the Technology Development Program (Project DST/TDT/TDP-03/2022).

AUTHOR DECLARATIONS

Conflict of Interest

The authors have no conflicts to disclose.

Author Contributions

A. K. N. developed the experimental setup and performed measurements. A. K. N. and V. K. participated in experiments, data analysis, numerical simulation, and data interpretation. G. K. S. developed the ideas and led the project. All authors

participated in the discussion and contributed to the manuscript writing.

DATA AVAILABILITY

The data that support the findings of this study are available from the corresponding author upon reasonable request.

References

- [1] M. Herrero-Collantes and J. C. Garcia-Escartin, “Quantum random number generators,” *Rev. Mod. Phys.*, vol. 89, p. 015004, Feb 2017.
- [2] F. James and L. Moneta, “Review of high-quality random number generators,” *Computing and Software for Big Science*, vol. 4, pp. 1–12, 2020.
- [3] Y. Dodis, D. Pointcheval, S. Ruhault, D. Vergnaud, and D. Wichs, “Security analysis of pseudo-random number generators with input: /dev/random is not robust,” Cryptology ePrint Archive, Paper 2013/338, 2013.
- [4] G. Brassard and C. Goutier, *Cryptologie contemporaine*. Paris Milan Mexico Masson, 1993, vol. 9.
- [5] H.-Q. Ma, Y. Xie, and L.-A. Wu, “Random number generation based on the time of arrival of single photons,” *Applied optics*, vol. 44, pp. 7760–3, 01 2006.
- [6] M. Stipčević and B. M. Rogina, “Quantum random number generator based on photonic emission in semiconductors,” *Review of Scientific Instruments*, vol. 78, no. 4, p. 045104, 04 2007.
- [7] F. Xu, B. Qi, X. Ma, H. Xu, H. Zheng, and H.-K. Lo, “Ultrafast quantum random number generation based on quantum phase fluctuations,” *Opt. Express*, vol. 20, no. 11, pp. 12 366–12 377, May 2012.
- [8] J. F. Dynes, Z. L. Yuan, A. W. Sharpe, and A. J. Shields, “A high speed, postprocessing free, quantum random number generator,” *Applied Physics Letters*, vol. 93, no. 3, p. 031109, 07 2008.
- [9] C. Gabriel, C. Wittmann, D. Sych, R. Dong, W. Mauerer, U. L. Andersen, C. Marquardt, and G. Leuchs, “A generator for unique quantum random numbers based on vacuum states,” *Nature Photonics*, vol. 4, no. 10, pp. 711–715, 2010.
- [10] S. Pironio, A. Acín, S. Massar, A. B. de La Giroday, D. N. Matsukevich, P. Maunz, S. Olmschenk, D. Hayes, L. Luo, T. A. Manning *et al.*, “Random numbers certified by bell’s theorem,” *Nature*, vol. 464, no. 7291, pp. 1021–1024, 2010.
- [11] A. Acín and L. Masanes, “Certified randomness in quantum physics,” *Nature*, vol. 540, pp. 213–219, 2016.
- [12] Y. Liu, Q. Zhao, M.-H. Li, J.-Y. Guan, Y. Zhang, B. Bai, W. Zhang, W.-Z. Liu, C. Wu, X. Yuan *et al.*, “Device-independent quantum random-number generation,” *Nature*, vol. 562, no. 7728, pp. 548–551, 2018.
- [13] J. F. Clauser, M. A. Horne, A. Shimony, and R. A. Holt, “Proposed experiment to test local hidden-variable theories,” *Phys. Rev. Lett.*, vol. 23, pp. 880–884, Oct 1969.
- [14] N. Leone, S. Azzini, S. Mazzucchi, V. Moretti, and L. Pavesi, “Certified quantum random-number generator based on single-photon entanglement,” *Phys. Rev. Appl.*, vol. 17, p. 034011, Mar 2022.
- [15] F. Xu, J. H. Shapiro, and F. N. C. Wong, “Experimental fast quantum random number generation using high-dimensional entanglement with entropy monitoring,” *Optica*, vol. 3, no. 11, pp. 1266–1269, Nov 2016.
- [16] B. G. Christensen, K. T. McCusker, J. B. Altepeter, B. Calkins, T. Gerrits, A. E. Lita, A. Miller, L. K. Shalm, Y. Zhang, S. W. Nam, N. Brunner, C. C. W. Lim, N. Gisin, and P. G. Kwiat, “Detection-loophole-free test of quantum nonlocality, and applications,” *Phys. Rev. Lett.*, vol. 111, p. 130406, Sep 2013.
- [17] Z. Cao, H. Zhou, X. Yuan, and X. Ma, “Source-independent quantum random number generation,” *Phys. Rev. X*, vol. 6, p. 011020, Feb 2016.
- [18] D. G. Marangon, G. Vallone, and P. Villoresi, “Source-device-independent ultrafast quantum random number generation,” *Phys. Rev. Lett.*, vol. 118, p. 060503, Feb 2017.

- [19] Z. Zheng, Y. Zhang, M. Huang, Z. Chen, S. Yu, and H. Guo, “Bias-free source-independent quantum random number generator,” *Opt. Express*, vol. 28, no. 15, pp. 22 388–22 398, Jul 2020.
- [20] A. K. Nai, A. Sharma, V. Kumar, S. Singh, S. Mishra, C. M. Chandrashekar, and G. K. Samanta, “Beamsplitter-free, high bit-rate, quantum random number generator based on temporal and spatial correlations of heralded single-photons,” 2024. [Online]. Available: <https://arxiv.org/abs/2410.00440>
- [21] Y. Yu, P.-F. Sun, Y.-Z. Zhang, B. Bai, Y.-Q. Fang, X.-Y. Luo, Z.-Y. An, J. Li, J. Zhang, F. Xu, X.-H. Bao, and J.-W. Pan, “Measurement-device-independent verification of a quantum memory,” *Phys. Rev. Lett.*, vol. 127, p. 160502, Oct 2021.
- [22] S. Pirandola, C. Ottaviani, G. Spedalieri, C. Weedbrook, S. L. Braunstein, S. Lloyd, T. Gehring, C. S. Jacobsen, and U. L. Andersen, “High-rate measurement-device-independent quantum cryptography,” *Nature Photonics*, vol. 9, no. 6, pp. 397–402, 2015.
- [23] L. Li, M. Cai, T. Wang, Z. Tan, P. Huang, K. Wu, and G. Zeng, “On-chip source-device-independent quantum random number generator,” *Photon. Res.*, vol. 12, no. 7, pp. 1379–1394, Jul 2024.
- [24] J. Cheng, S. Liang, J. Qin, J. Li, Z. Yan, X. Jia, C. Xie, and K. Peng, “Semi-device-independent quantum random number generator with a broadband squeezed state of light,” *npj Quantum Information*, vol. 10, no. 1, p. 20, 2024.
- [25] X. Chen, J. N. Greiner, J. Wrachtrup, and I. Gerhardt, “Single photon randomness based on a defect center in diamond,” *Scientific Reports*, vol. 9, no. 1, p. 18474, Dec 2019.
- [26] B. Haylock, D. Peace, F. Lenzini, C. Weedbrook, and M. Lobino, “Multiplexed Quantum Random Number Generation,” *Quantum*, vol. 3, p. 141, May 2019.
- [27] M. V. Jabir and G. K. Samanta, “Robust, high brightness, degenerate entangled photon source at room temperature,” *Scientific Reports*, vol. 7, no. 1, p. 12613, Oct 2017.
- [28] S. Singh, V. Kumar, A. Ghosh, A. Forbes, and G. K. Samanta, “A tolerance-enhanced spontaneous parametric downconversion source of bright entangled photons,” *Advanced Quantum Technologies*, vol. 6, no. 2, p. 2200121, 2023.
- [29] X. Ma, F. Xu, H. Xu, X. Tan, B. Qi, and H.-K. Lo, “Postprocessing for quantum random-number generators: Entropy evaluation and randomness extraction,” *Phys. Rev. A*, vol. 87, p. 062327, Jun 2013.
- [30] H. Krawczyk, “Lfsr-based hashing and authentication crypto’94 (lecture notes in computer science vol 839) ed desmedt y,” 1994.
- [31] A. Rukhin, J. Soto, J. Nechvatal, M. Smid, E. Barker, S. Leigh, M. Levenson, M. Vangel, D. Banks, A. Heckert *et al.*, *A statistical test suite for random and pseudorandom number generators for cryptographic applications*. US Department of Commerce, Technology Administration, National Institute of . . . , 2001, vol. 22.
- [32] P. L’ecuyer and R. Simard, “Testu01: A library for empirical testing of random number generators,” *ACM Transactions on Mathematical Software (TOMS)*, vol. 33, no. 4, pp. 1–40, 2007.
- [33] M. E. O’neill, “Pcg: A family of simple fast space-efficient statistically good algorithms for random number generation,” *ACM Transactions on Mathematical Software*, 2014.